Recoil of products from reactions of ^{20,22}Ne with ^{93}Nb at 100 and 142 MeV

J. J. Hogan
Department of Chemistry, McGill University, Montreal, Quebec, Canada
and Nuclear Physics Division, Atomic Energy Research Establishment Harwell, Oxfordshire, United Kingdom

J. Asher and D. J. Parker
Nuclear Physics Division, Atomic Energy Research Establishment Harwell, Oxfordshire, United Kingdom
(Received 2 November 1984)

The recoil properties of thirty-five nuclides produced in reactions of 100 and 142 MeV ^{20}Ne and ^{22}Ne with ^{93}Nb have been measured. A thick-target/thick-catcher technique was used, with the foils mounted at 45° to the beam axis so as to provide information on the transverse as well as the longitudinal momentum transfer. Relationships have been derived to extract values, from the resulting data, for the average longitudinal component of recoil velocity and the average recoil angle. The experimental results show, in almost all cases, mean recoil velocities less than the compound nuclear velocity. For products with near-target mass, transverse momentum transfers greater than those along the axis were observed. For heavier products, the momentum transfer increases with the product mass. The results from the ^{22}Ne-induced reactions are significantly different from those of ^{20}Ne. The results are interpreted mainly in terms of two competing mechanisms: complete fusion/evaporation and a class of process involving varying degrees of mass transfer between projectile and target.

I. INTRODUCTION

Nuclear reactions induced by "light" heavy ions ($2 < Z < 11$) at energies up to 10 MeV/nucleon have been studied for more than two decades.[1–3] The mechanisms of these reactions may be broadly classified between two extremes: reactions involving complete fusion of projectile and target, followed by particle evaporation, and direct transfer reactions. At these energies, simple one-step transfer processes are less important than transfer processes involving transfer to the continuum with subsequent evaporation, and a variety of processes between the two extremes involving partial mass transfer with or without substantial excitation of the resulting intermediate nucleus may exist. A given reaction often involves contributions from two or more distinct mechanisms.

Three basic aspects of complete fusion, which are all related to the potentially large angular momentum of the fused system, are generally studied: (a) the probability for forming the fused system, as a function of excitation energy and angular momentum,[4,5] (b) the nature of the deexcitation processes from high spin states, including yrast trapping and the enhanced emission of clusters of nucleons,[6] and (c) the nuclear properties of high spin states, including nuclear shapes, rotational energies, etc.[7]

Theoretical studies of transfer processes have concentrated on the mechanisms involved in the flow of nuclear matter.[8,9] Frequently overlapping terminology for these phenomena has come into common usage: incomplete fusion, deep inelastic scattering, damped collisions, quasifission, multistep direct and compound processes, and the all-encompassing preequilibrium reactions.[10] Many classical analogs have been invoked in order to describe the features of these reactions, such as diffusion, "hot spots," viscosity, and parameters like tangential and rolling friction.

Most of the experimental studies on which these theories have been based have comprised measurements of double-differential particle spectra of emitted fragments,[11] often in coincidence with either the projectile or its remains following interaction. Relatively little work has looked specifically at the recoil properties of the heavy reaction product (the "residue"), although in many situations this may be used to characterize the mechanism.

Many of the mechanisms already listed occur in two stages, where the first stage leads to formation of a recoiling excited intermediate, accompanied by a projectilelike fragment or fragments, and the second stage consists of deexcitation of the intermediate by means of particle evaporation. If the evaporation process is symmetric about 90°, the average recoil velocity and angle of the final residue will be identical to those of the intermediate nucleus. Moreover, the end of the first stage may usually be treated as a two-body state, so that knowledge of the recoil velocity and angle of a selected intermediate determines the energy and angle of emission of the accompanying projectilelike fragment. In cases where more than one fragment is emitted, what is determined is the motion of the common center of mass of the fragments. The net excitation energy of the intermediate plus the fragments is also determined; in general, this is expected to appear mainly as excitation of the intermediate, although, where more than one fragment is involved, the separation energy and relative kinetic energy of the individual fragments are also included. Provided that a particular residue is formed by a single such mechanism, measurement of its average recoil velocity and angle may enable the intermediate to be identified by means of this type of analysis.

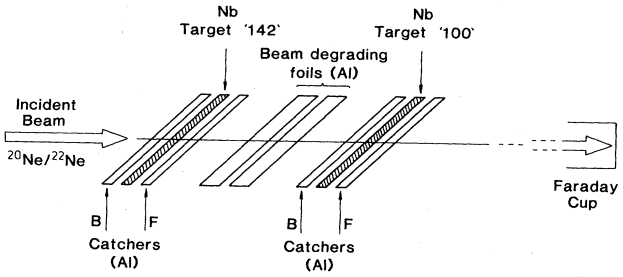

FIG. 1. Experimental arrangement for irradiation of the foil stacks, mounted at 45° to the beam axis. Each niobium target is sandwiched between two catchers, a forward catcher, labeled "*F*," and a backward catcher, labeled "*B*."

For radioactive products, measurement of the recoil range of the residue in a stopping medium is a well-established method for obtaining information on the recoil velocity.[12] Although the Orsay group has made extensive use of such recoil techniques in studying quasielastic and deep inelastic processes on heavy targets,[13] and various studies have been made at relativistic energies,[14] the full potential of recoil range techniques has not in general been exploited. Recently, Parker *et al.*[15] have demonstrated the value of detailed analysis of differential recoil range distributions in investigations of complete and incomplete fusion. The present work extends the use of simple recoil techniques in reaction studies. Whereas most previous studies have generally measured either the (mean) projected recoil range (which reflects only the longitudinal component of the recoil velocity) or the recoil angular distribution, the present work used a catcher/target/catcher stack mounted at 45° to the beam axis, enabling (in favorable cases) simultaneous determination of both the mean projected range and the approximate recoil angle, and hence, the longitudinal and transverse momentum transfer. This is possible only for recoil angles greater than 45°, corresponding to products formed in glancing collisions. However, for products with small recoil angles, the projected range alone (as measured in previous studies) is sufficient to characterize the reaction.

The target nucleus chosen was ^{93}Nb. Many of the possible products of reactions of light heavy ions with this target are radionuclides having half-lives and decay properties suitable for off-line measurements. In particular, this target is appropriate for studying transfer processes, since the products of alpha transfer from projectile to target are the well-known isomers of the technetium isotopes, while mass transfers from target to projectile produce a wide range of conveniently measurable products.

Two projectiles were chosen: ^{20}Ne and ^{22}Ne. These may be considered to bridge the region between ^{12}C, whose reactions are largely understandable in terms of a composite of three alpha particles (see, for example, Ref. 15), and the heavy ions from Ar up, in which projectile structure effects play little role in the overall reaction. In addition, ^{20}Ne retains the flavor of an alpha-composite nucleus, while ^{22}Ne has two extra neutrons. The somewhat different results from the two systems will be compared in the appropriate sections of this work.

The projectile energies chosen, about 100 and 142 MeV, correspond, respectively, to an incident energy a little above the Coulomb barrier, and an energy which approximates that for which the critical angular momentum[16,17] for complete fusion may be exceeded. Recoil properties have been measured for a total of thirty-five product residues; the results of four sets of measurements, with both projectiles at both energies, are presented here.

A study of the recoil properties of products from the interactions of 142 MeV ^{20}Ne with ^{93}Nb has previously been made by Shaw and Smith of Manchester.[18,19] The present work considerably extends the scope and detail of these studies.

Section II describes the experimental arrangement used. In Sec. III, the recoil equations required to analyze the results are derived and discussed. The results obtained and their implications for the reaction mechanisms are discussed in Sec. IV.

II. EXPERIMENTAL PROCEDURE

A. Target stacks

The target stacks consisted of 99.9% pure Nb metal foils, nominally 0.003 mm thick, and 99.7% pure Al metal foils, ranging from 0.002 to 0.005 mm thick, all obtained from Goodfellow Metals of Cambridge, England. These were arranged to provide catcher foils of Al upstream and downstream of each of two targets, separated by sufficient Al foils to degrade the average energy of the Ne beams to that required for the second target (see Fig. 1). Two stacks were used, one for ^{20}Ne and one for the ^{22}Ne measurement.

Nominal thicknesses of foils appropriate to the energy requirements were calculated using the range tables of Northcliffe and Schilling.[20] The actual thicknesses were measured by cutting to size and weighing. The components of each of the target stacks are listed in Table I.

The target arrangement was unique to this experiment. Since the aim was to measure the perpendicular as well as the parallel component of the momentum transfer in the reaction, the entire stack was mounted at an angle of 45° to the beam axis, increasing the effective thickness of each foil by $\sqrt{2}$. The target thickness in the case of the ^{20}Ne measurements was 2.65 mg/cm^2, yielding an effective thickness at this angle of 3.75 mg/cm^2; for the ^{22}Ne measurements the target thickness was 2.75 mg/cm^2, giving an effective thickness of 3.89 mg/cm^2. The energy losses listed in Table I were calculated[20] using the effective target thickness.

The two catchers associated with each target will be referred to, for convenience, as the corresponding "forward" and "backward" catchers, respectively, as shown in Fig. 1.

B. Beams and irradiations

Two irradiations were carried out using beams extracted from the Harwell Variable Energy Cyclotron. The beam for the ^{20}Ne experiments was obtained from unenriched neon gas, while the ^{22}Ne beam was obtained from neon enriched to approximately 20% in ^{22}Ne. Both

TABLE I. Target stacks.

Beam energy (MeV)	Foil	Effective thickness (mg/cm^2)	Function
		^{20}Ne	
150.0			
	Al	0.76	backward catcher
147.0			
	Nb	3.75	target
136.0			
	Al	1.91	forward catcher
127.8			
	Al	1.91	degrader
119.2			
	Al	1.91	degrader
110.2			
	Al	0.76	backward catcher
106.5			
	Nb	3.75	target
93.2			
	Al	1.91	forward catcher
82.7			
		^{22}Ne	
151.8			
	Al	0.76	backward catcher
148.6			
	Nb	3.89	target
136.6			
	Al	1.91	forward catcher
127.9			
	Al	1.91	degrader
118.8			
	Al	1.91	degrader
109.2			
	Al	0.76	backward catcher
105.3			
	Nb	3.89	target
90.7			
	Al	1.91	forward catcher
79.5			

beams were in the 6^+ charge state; the beam energies at the point of entry to the target stack were 150.0 and 151.8 MeV, respectively. The beam intensity in the ^{20}Ne experiment averaged about 35 nA throughout a 5 h irradiation. Because of the low enrichment, the ^{22}Ne beam intensity was only about 5 nA; the irradiation time was again about 5 h.

The incident beam energies provided an average beam energy within the target layer of about 142 MeV in the upstream stack and about 100 MeV in the downstream stack (see Table I). It should be noted that each target actually covered a considerable range of beam energy (more than 10 MeV). For convenience, the energies are referred to here as 142 and 100 MeV.

C. Counting procedures

After irradiation, the target stack was disassembled, and the individual foils counted repeatedly at a distance of approximately 25 mm from the face of a Ge(Li) detector with an absolute gamma-ray photopeak efficiency, in this geometry, of about 5% at 150 keV, decreasing logarithmically to about 0.4% at 2000 keV. Using the half-lives, gamma-ray energies and, where necessary, branching ratios taken from the GSI Gamma Ray Catalog,[21] the yields of a variety of nuclides produced in the reactions were determined for the two target foils and four catcher foils of each stack. The decay curves measured in this way were then analyzed by a least-squares procedure to determine the activity present at the end of irradiation. In one of the degrader foils, counted as a blank, no activities other than those attributable to reactions of Ne on Al were found. In these studies, we are concerned only with comparing the relative yields for each nuclide in the target and catchers; systematic uncertainties in the decay characteristics are therefore eliminated.

The nuclides studied are listed in Table II with their pertinent decay characteristics. This study is complicated by the possible presence of "feeding" of the observed nuclides, so that the nuclide observed may not in some cases be the actual reaction product, but one of its β-decay daughters. The designations CUM (for cumulative) and IND (for independent) relate to the possibility of feeding. CUM means that the nuclide may have been fed from beta-decaying precursors, while IND means that the nu-

TABLE II. Decay characteristics of nuclides studied in this work.

Nuclide	Half-life	Gamma energy (keV)	Mode
^{87}Y^m	13.0 h	381.0	CUM
^{88}Zr	83.4 d	392.9	CUM
^{89}Zr^g	78.4 h	909.2	CUM
^{90}Mo	5.67 h	257.3	CUM
^{90}Nb^g	14.6 h	1129.7	IND
^{92}Nb^m	10.13 d	934.5	IND
^{93}Mo^m	6.9 h	263.1	IND
^{93}Tc^g	2.73 h	1362.9	CUM
^{94}Tc^g	4.88 h	871.0	CUM
^{95}Nb^g	3.50 d	765.8	IND
^{95}Tc^g	20.0 h	765.8	CUM
^{96}Tc^{m,g}	4.3 d	778.2	IND
^{97}Rh^g	31 min	421.5	CUM
^{98}Rh^g	8.7 min	652.0	CUM
^{99}Rh^m	4.7 h	340.6	CUM
^{100}Rh^g	21.0 h	539.6	CUM
^{100}Pd	3.7 d	539.6	CUM
^{101}Ag^g	11.4 min	263.0	CUM
^{101}Pd	8.5 h	296.3	CUM
^{102}Ag^g	13.0 min	1744.6	CUM
^{103}Ag^g	1.10 h	118.7	CUM
^{104}Ag^g	68.5 min	555.8	CUM
^{104}Cd	57.7 min	709.3	CUM
^{105}Ag^{m,g}	41.3 d	344.5	CUM
^{105}Cd	55.5 min	961.8	CUM
^{106}In^{m,g}	6 min	632.7	CUM
^{107}In^g	32.4 min	205.0	CUM
^{108}In^a	58.0 min	633.0	CUM
^{108}Sn	10.5 min	397.1	CUM
^{109}In^g	4.2 h	347.4	CUM
^{109}Sn^g	18.0 min	1098.1	CUM
^{110}In^m	4.9 h	883.4	IND
^{110}Sn	4.0 h	280.2	CUM
^{111}In^g	2.83 d	245.4	CUM
^{111}Sn	35.3 min	1152.4	CUM

[a]It was not possible experimentally to distinguish ground state from metastable state.

clide is shielded (flanked by stable isobars), has a long-lived parent, or has a parent that cannot be produced in these reactions.

III. ANALYSIS

The velocity and direction of recoil of a reaction residue reflect the mechanism responsible for its formation. In a thick-target/thick-catcher study, such as the present work, the residue finally stops in either the target foil itself or a catcher foil, depending upon the range of the product in the target material and its angle of recoil. Thus the relative yields of a given product in the target and catchers provide information on the recoil velocities and angles involved.

This paper reports measurements using a catcher/target/catcher stack mounted at 45° to the beam axis, as shown in Fig. 1. The nomenclature "forward" and "backward" is used to denote the position of the two catchers, although, by virtue of the 45° mounting angle, much of the backward catcher is actually downstream of much of the forward catcher. No reaction products are expected to travel backwards; instead, the backward catcher is designed to stop products traveling forward with recoil angles greater than 45°. These products will also be found in the forward catcher and the target foil, while products traveling forward with recoil angles less than 45° will be found exclusively in the forward catcher and the target foil. For recoil angles between 45° and 90°, the total yield in the forward catcher is always larger than that in the backward catcher.

The measurements described in the preceding section provide, for each product studied, the two quantities f_F and f_B, the fractions of the total yield found, respectively, in the forward and backward catchers. In this section, it will be shown how these measured quantities are related to the average recoil velocity and angle of the residue.

In the derivation of the recoil equations, it will be assumed that:

(i) The effective target thickness T is greater than the longest range of any product.

(ii) The reaction mechanism is cylindrically symmetric about the beam axis.

Further assumptions necessary to interpret the results will be introduced as required.

The origins of the two expressions used can be seen by considering the case of a unique recoil velocity and angle. Suppose that the product of interest recoils at an angle α to the beam axis ($0° < \alpha < 90°$) with a velocity v, for which the corresponding range in niobium is R. The components of R, parallel and perpendicular to the beam axis, are defined as $R_{||} = R\cos\alpha$ and $R_{\perp} = R\sin\alpha$. When all possible points of origin in the target and all possible orientations of the recoil velocity are considered, the final yield is distributed over the curved surface of a circular cylinder of radius $R_{\perp}$ and length T, as shown in Fig. 2.

If the target stack is mounted normal to the beam axis, as in Fig. 2(a), the fraction f_F of the yield that escapes into the forward catcher is equal to $R_{||}/T$. The result is the same if the stack is turned to 45°, provided that $R_{||} > R_{\perp}$, as shown schematically in Fig. 2(b), because the additional yield that escapes from one-half of the target is exactly balanced by that trapped in the target from the other half [represented by the two shaded regions in Fig. 2(b)]. The target thickness T is now the effective thickness measured along the beam axis.

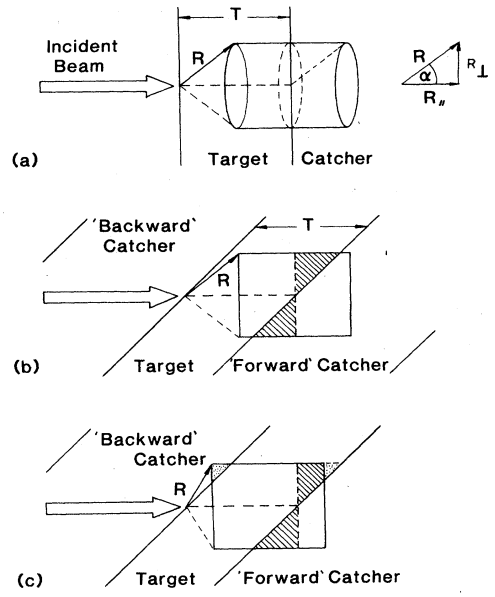

FIG. 2. The geometric basis for derivation of the recoil equations, for a reaction product with unique recoil range, R, and recoil angle, α, generated throughout the target. The locus of ends of range of the product, a cylinder of length T, radius $R_{\perp}$, is shown for a target normal to the beam axis (a), and for a target at 45° to the beam axis, where $\alpha < 45°$ (b), and where $\alpha > 45°$ (c).

If, however, $R_{\perp} > R_{||}$, as in Fig. 2(c), it is no longer true that the extra yield trapped in one-half of the target is equal to that escaping forward from the other half, since a portion of the cylinder [shown dotted on the right of Fig. 2(c)] is missing. Moreover, part of the yield, given by the area of the cut off portion, now enters the backward catcher. Then $f_F - f_B = R_{||}/T$, and hence,

$$R_{||} = T(f_F - f_B) \,. \tag{1}$$

In order to determine $R_{\perp}$ or α, it is necessary to evaluate the fraction of the yield in the cutoff corner of the cylinder. The area of the curved surface cut off is

$$2R_{\perp}[(R_{\perp}^2 - R_{||}^2)^{1/2} - R_{||}\cos^{-1}(R_{||}/R_{\perp})] \,,$$

whereas the total curved surface area of the cylinder is simply $2\pi R_{\perp} T$. Hence,

$$f_B = [(R_{\perp}^2 - R_{||}^2)^{1/2} - R_{||}\cos^{-1}(R_{||}/R_{\perp})]/\pi T \,,$$
$$= R_{||}[(\tan^2\alpha - 1)^{1/2} - \cos^{-1}(\cot\alpha)]/\pi T \,,$$

where α is the recoil angle, and so, from (1),

$$\frac{\pi f_B}{f_F - f_B} = (\tan^2\alpha - 1)^{1/2} - \cos^{-1}(\cot\alpha) \,. \tag{2}$$

Provided $f_B > 0$, this transcendental equation may be solved for the angle α.

The preceding discussion above has treated the products as if their entire recoil path occurred in niobium. In practice, at some stage, some of the products escape into one or other of the aluminum catchers, in which the stopping power is different. This does not, however, affect the expressions obtained for the fractions of the yield escaping from the target foil.

In practice, the measured quantities, $T(f_F - f_B)$ and $\pi f_B/(f_F - f_B)$, represent average values (over the recoil distribution) of $R_{||}$ and $[(\tan^2\alpha - 1)^{1/2} - \cos^{-1}(\cot\alpha)]$. These average quantities are useful provided that the width of the distribution of range vectors is relatively narrow; as discussed later, if the distribution of angles α is broad (due, for example, to the effects of evaporation or nuclear straggling during the stopping process), care must be taken in interpreting the value obtained for α.

A. The parallel range component, $R_{||}$

From Eq. (1), for any distribution of recoil velocities, the quantity $T(f_F - f_B)$ is equal to $\bar{R}_{||}$, the average value of the parallel component of the range. Physically, however, one is more interested in the parallel velocity component, $v_{||}$. Conversion from range to velocity requires knowledge of the range/energy relationship for the product concerned in niobium. If the range were directly proportional to velocity, one could obtain the mean value of the projected velocity, $\bar{v}_{||}$, directly from $\bar{R}_{||}$. While this is not in general the case, it is generally true that over a reasonably narrow velocity interval the range is an approximately linear function of velocity, so that for a distribution of velocities v it is still possible to obtain $\bar{v}$ directly from $\bar{R}$. However, where the recoil angle is large, it is not sufficient to use $\bar{R}_{||}$ to obtain $\bar{v}_{||}/\cos\alpha$; instead, one must first obtain an estimate of the total range $\bar{R} = \bar{R}_{||}/\cos\alpha$, derive from this the corresponding velocity $\bar{v}$, and form from this the longitudinal component $\bar{v}_{||} = \bar{v}\cos\alpha$.

Accordingly, in the present work, from the measured values of f_F and f_B, the mean parallel range component $\bar{R}_{||}$ has been calculated from $\bar{R}_{||} = T(f_F - f_B)$. In cases where no yield was found in the backward catcher, indicating recoil angles less than 45°, this range component has been directly converted to the velocity component $\bar{v}_{||}$, but where a value for the recoil angle α was obtained, this was used in the derivation of $\bar{v}_{||}$ from $\bar{R}_{||}$ (the corrected value $\bar{\alpha}_c$, as discussed in Sec. III B, was in fact used). Taking the value of $\bar{R}_{||}$ alone would have led to estimates for $\bar{v}_{||}$ higher than those given by between 15% (for $\bar{\alpha}_c \simeq 45°$) and 50% (for $\bar{\alpha}_c \simeq 65°$), indicating the importance, even in studies of $\bar{v}_{||}$, of determining α, where this is large.

For the range/energy relationship, a local parabolic parametrization of the relevant table of Northcliffe and Schilling[20] was used, applying mass scaling for isotopes other than those listed, to provide the energy E corresponding to range $\bar{R}_{||}$ or $\bar{R}$ as appropriate. The values obtained for $\bar{R}_{||}$ and E are listed in Tables III and IV. From E, and $\bar{\alpha}$ as appropriate, a value of $\bar{v}_{||}$ was calculated for each product. The results will be discussed in Sec. IV, where they are presented as a fraction of the full compound nuclear (cn) velocity

$$V_{\rm cn} = \sqrt{2A_{\rm p}E_{\rm p}}/A_{\rm cn} ,$$

where $A_{\rm p}$ and $A_{\rm cn}$ denote the masses of projectile and compound nucleus, respectively, and $E_{\rm p}$ denotes the projectile laboratory energy.

For comparison, the values of $\bar{R}_{||}$ obtained using 142 MeV ^{20}Ne by Shaw and Smith[18,19] are also listed in Tables III and IV; these agree quite well with corresponding results from the present work.

B. The recoil angle, α

It has already been noted that Eq. (2) applies only if the final recoil angle $\alpha > 45°$; otherwise $f_B = 0$. Hence, for a distribution of velocities, the quantity

$$\pi f_B/(f_F - f_B)$$

is equal to the weighted average of the expression

$$[(\tan^2\alpha - 1)^{1/2} - \cos^{-1}(\cot\alpha)]$$

taken only over processes with $\alpha > 45°$, other processes contributing zero.

This expression depends only upon the distribution of angles and is not affected at all by the magnitude of the recoil velocity or the nature of the range/energy relation.

In general, where there is a distribution of angles, the value of $\bar{\alpha}$ obtained by solving the transcendental equation

$$\pi f_B/(f_F - f_B) = (\tan^2\bar{\alpha} - 1)^{1/2} - \cos^{-1}(\cot\bar{\alpha})$$

is not simply related to the mean recoil angle. If the recoil velocity distribution is narrowly defined in angle, the value of $\bar{\alpha}$ obtained closely approximates the mean recoil angle. If, however, the distribution is significantly broadened, it can be shown that the value of $\bar{\alpha}$ obtained is systematically increased because of the biasing effect of the nonlinearity of the preceding expression. Furthermore, if the distribution extends below 45°, the averaging process is truncated, giving an additional systematic increase in $\bar{\alpha}$.

Three broadening contributions have been considered:

(i) *Evaporation from a well-defined intermediate, which perturbs the original recoil velocity v_0 by an additional velocity, u.* (See Fig. 3.) Provided that the evaporation is symmetric about 90°, it can be shown that, to first order in (u/v_0), the value of $\bar{\alpha}$ is equal to the original recoil angle α_0, when $\alpha_0 \gg 45°$. In the case of those processes studied here for which products were found in the backward catcher, so that $\bar{\alpha}$ could be estimated, evaporation of only a very few nucleons is expected to occur; the resulting perturbation in the recoil velocity is small and amounts to only a few degrees spread in α.

(ii) *Transverse range straggling, mainly due to nuclear stopping, which further broadens the distribution of final recoil angles.* The values of $\bar{R}_{||}$ and $\bar{\alpha}$ found here for products with some yield in the backward catcher imply

TABLE III. Observed recoil properties of high-mass products. (All ranges in mg/cm^2 of niobium, all energies in MeV.)

Nuclide	^{20}Ne 141.5 MeV		^{20}Ne 142 MeV (Shaw and Smith)		^{22}Ne 142.6 MeV		^{20}Ne 99.9 MeV		^{22}Ne 98.0 MeV	
	$\bar{R}_{\|\|}$	E	$\bar{R}_{\|\|}$	E	$\bar{R}_{\|\|}$	E	$\bar{R}_{\|\|}$	E	$\bar{R}_{\|\|}$	E
^{97}Rh^{g}	1.24±0.21	7.0±1.4								
^{98}Rh^{g}	1.50±0.07	8.9±0.5								
^{99}Rh^{m}	1.90±0.08	12.2±0.7			1.21±0.06	6.7±0.4	0.74±0.03	3.9±0.2		
^{100}Rh^{g}	1.93±0.02	12.4±0.2			1.59±0.12	9.5±0.9	1.10±0.01	6.0±0.1		
^{100}Pd	2.08±0.01	15.4±0.1			1.50±0.15	9.8±1.2				
^{101}Ag^{g}	2.04±0.38	13.9±3.5								
^{101}Pd	2.27±0.04	17.5±0.4			1.63±0.08	10.9±0.7				
^{102}Ag^{g}	2.22±0.11	15.6±1.1	2.31	16.6						
^{103}Ag^{g}	2.13±0.12	14.7±1.1	2.38	17.2	1.97±0.06	13.1±0.5	1.44±0.12	8.7±0.9		
^{104}Ag^{g}	2.30±0.14	16.3±1.4	2.37	17.1			1.59±0.21	9.8±1.6		
^{104}Cd	2.34±0.10	17.3±1.0			1.76±0.33	11.6±2.7				
^{105}Ag^{m,g}	2.53±0.02	18.7±0.2	2.57	19.2	1.99±0.10	13.2±0.9	1.59±0.03	9.8±0.2		
^{105}Cd	2.35±0.41	17.3±4.1			2.30±0.25	16.8±2.5	1.30±0.29	7.9±1.9	1.68±0.31	10.9±2.4
^{105}In			2.45	18.8						
^{106}In^{m,g}	2.85±0.05	20.2±0.6	2.71	21.8						
^{107}In^{g}	2.57±0.09	20.0±1.0	2.63	20.7	2.32±0.06	17.2±0.6	1.89±0.09	12.9±0.8	0.82±0.16	5.1±0.8
^{108}In^{a}	2.84±0.09	23.2±1.1	2.55	19.7	2.23±0.08	16.2±0.8	2.25±0.14	16.4±1.4	1.26±0.02	7.8±0.1
^{108}Sn	2.91±0.19	24.7±2.2	2.67	21.7			1.46±0.08	9.4±0.6		
^{109}In^{g}	2.66±0.09	20.9±1.1	2.59	20.0	2.53±0.03	19.4±0.3	2.08±0.03	14.6±0.3	1.61±0.03	10.4±0.2
^{109}Sn^{g}					2.40±0.39	18.4±4.0	1.99±0.07	14.1±0.6		
^{110}In^{m}					2.81±0.18	22.6±2.1			1.07±0.08	6.5±0.5
^{110}Sn					2.92±0.06	24.6±0.7			0.98±0.02	6.0±0.1
^{111}In^{g}					3.00±0.11	24.9±1.4			1.49±0.11	9.4±0.8
^{111}Sn									1.56±0.11	10.2±0.8

[a]It was not possible experimentally to distinguish ground state from metastable state.

TABLE IV. Observed recoil properties of low-mass products. All ranges in mg/cm^2, angles in degrees, energies in MeV.

	^{20}Ne 141.5 MeV				^{20}Ne 142 MeV (Shaw and Smith)	^{22}Ne 142.6 MeV				^{20}Ne 99.9 MeV			
	$\bar{R}_{\|\|}$	$\bar{\alpha}$	$\bar{\alpha}_c$	$\bar{R}$	E	$\bar{R}_{\|\|}$	$\bar{\alpha}$	$\bar{\alpha}_c$	$\bar{R}$	E	$\bar{R}_{\|\|}$	$\bar{\alpha}$	$\bar{\alpha}_c$	$\bar{R}$	E
^{87}Y^m	0.68±0.02	57.0±0.8	54±1	1.16±0.05	5.6±0.3	0.84	0.71±0.14	59.0±2.0	56±2	1.27±0.28	6.3±1.7				
^{88}Zr	0.76±0.09	55.8±3.1	53±3	1.26±0.20	6.4±1.3										
^{89}Zr^g	0.42±0.02	57.8±1.2	55±2	0.73±0.06	3.4±0.3	0.91	0.39±0.06	64.4±3.7	61±4	0.80±0.20	3.7±1.0	0.22±0.03	78.1±2.2	68±3	0.59±0.12	2.6±0
^{90}Nb^g	0.44±0.02	56.2±0.8	53±1	0.73±0.04	3.5±0.3	0.50										
^{92}Nb^m	0.28±0.02	72.8±1.0	66±2	0.69±0.08	3.2±0.4		0.26±0.03	75.4±2.2	67±3	0.67±0.12	3.1±0.7	0.33±0.04	64.4±1.0	61±2	0.68±0.10	3.2±0
^{93}Mo^m	0.49±0.01	52.4±0.4	49±1	0.75±0.03	3.6±0.2	0.59	0.43±0.02	55.8±1.2	53±2	0.71±0.05	3.4±0.3	0.37±0.05	61.6±1.8	58±2	0.70±0.11	3.4±0
^{93}Tc^g	0.56±0.01	50.3±1.0	46±1	0.81±0.03	4.0±0.2		0.53±0.25	59.0±2.1	56±2	0.95±0.45	4.9±2.7					
^{94}Tc^g	0.56±0.01	50.6±0.4	46±1	0.81±0.03	4.0±0.2	0.57						0.43±0.04	58.6±0.8	55±1	0.75±0.08	3.7±0
^{95}Nb^g							0.44±0.02	62 ±17	59±17	$0.8^{+1.0}_{-0.4}$	$4.1^{+6.5}_{-2.0}$					
^{95}Tc^g	0.57±0.01	51.3±0.4	47±1	0.84±0.03	4.2±0.2	0.52	0.51±0.06	53.9±2.0	51±2	0.81±0.12	4.1±0.7	0.58±0.01	55.8±0.4	53±1	0.96±0.04	4.9±0
^{96}Tc^{m,g}	0.60±0.01	51.3±0.4	47±1	0.88±0.03	4.5±0.2	0.59	0.59±0.03	52.0±1.1	48±2	0.88±0.06	4.5±0.4	0.77±0.01	53.9±0.4	51±1	1.22±0.04	6.6±0

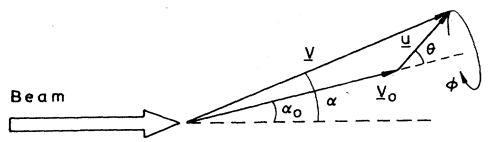

FIG. 3. Velocity vector diagram, illustrating the effect of a perturbing velocity, u, due, for example, to light particle evaporation, on the initial recoil velocity, v_0, resulting in the final velocity, v.

mean recoil energies of 3—8 MeV. At these energies, the estimated standard deviation of the transverse range distribution due to straggling is about 20% of the range;[22] this implies a spread (assumed Gaussian) in the distribution of α, with a 12° standard deviation, resulting in a significant overestimate of $\bar{\alpha}$.

(iii) *The angular distribution arising from the distribution of impact parameter and/or the spread in reaction Q values/excitation energies involved.* This is the most difficult contribution to estimate; however, in the reactions studied here, it is probably considerably less significant than (ii), but may be comparable to (i).

Of these three factors, all of which lead to broadening of the distribution of angles α and hence to a systematic overestimate of the mean angle $\bar{\alpha}$, (ii) is the most significant. Accordingly we have corrected the measured values of $\bar{\alpha}$ for the systematic shift due to a three-dimensional Gaussian distribution of end points with a standard deviation of 12° in angle, following the calculations of Littmark and Ziegler[22] for the transverse straggling. The corrected values $\bar{\alpha}_c$ are listed in Table IV, together with the original measured values $\bar{\alpha}$. The uncertainties in $\bar{\alpha}$ listed arise from statistical uncertainties in f_F and f_B, but the dominant uncertainty in the values of $\bar{\alpha}_c$ is likely to arise in the correction for the systematic overestimate; a systematic uncertainty of 5—10% in the corrected values is possible. No correction has been attempted to account for (i) or (iii).

IV. DISCUSSION OF RESULTS

The analysis described in Sec. III yields values of $\bar{v}_{||}$ for all observed products, and of the recoil angle $\bar{\alpha}_c$ for products with $\alpha > 45°$ (those found in the backward catcher). In the present work, the only products found in the backward catcher were those with mass $A \leq 96$. It is noteworthy that virtually all the observed products with $A \leq 96$ were found with significant yield in the backward catcher, indicating that these low mass products are formed in glancing collisions involving large recoil angles. A full discussion of the implications of the low mass results will be given separately, following the general discussion based on the values of $\bar{v}_{||}$ alone.

A. $\bar{v}_{||}$ results

The values for $\bar{v}_{||}$ obtained in the four sets of measurements are shown as a function of product mass A in Fig. 4. The following discussion treats the 142 MeV data for ^{20}Ne and ^{22}Ne as well as the 100 MeV ^{20}Ne data. The few

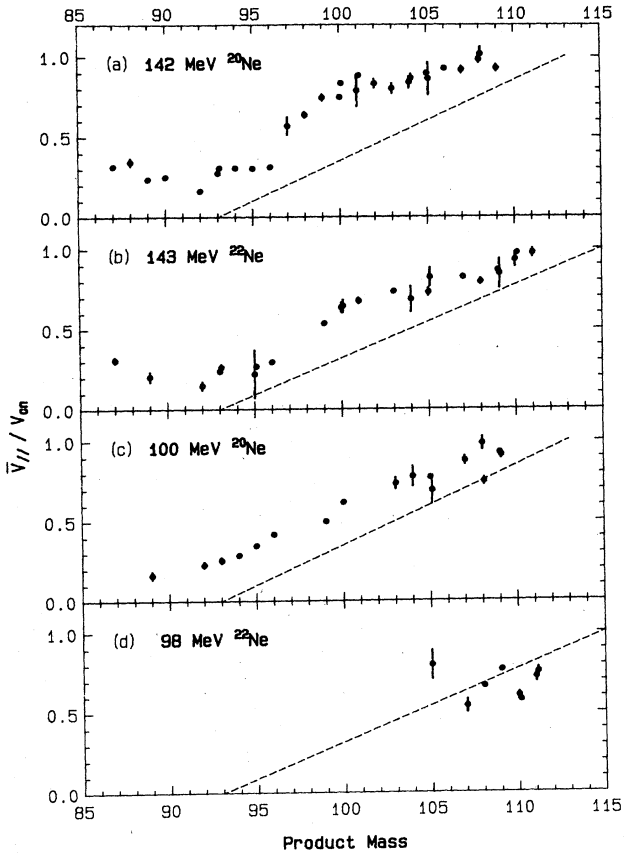

FIG. 4. Ratio of the mean velocity component parallel to the beam axis, $v_{||}$, to the compound nuclear velocity, v_{cn} (assuming complete fusion) for detected products from the reactions of ^{20}Ne and ^{22}Ne with ^{93}Nb, as a function of product mass. The dashed lines represent the velocity ratios, as a function of their masses, for reaction intermediates formed by breakup/incomplete fusion.

results obtained with 100 MeV ^{22}Ne show somewhat different behavior, which will be briefly discussed later.

It is apparent from Fig. 4 that, for the heaviest observed products, the value of $\bar{v}_{||}$ is between 90% and 100% of the compound nuclear velocity in each case, but decreases steadily as the product mass decreases, to a value of only about $0.2v_{cn}$ for products close to the target. In the two sets of 142 MeV data, there is some evidence that $\bar{v}_{||}$ increases again with increasing ΔA below the target mass.

The absolute values obtained for $\bar{v}_{||}$ for a given element depend upon the range/energy relation of Northcliffe and Schilling[20] and may be systematically in error by perhaps 10%. Trends in the data are thus much more significant than absolute values, and little weight should be attached to the observation that the results for the heaviest products level out at about $0.93v_{cn}$, rather than $1.0v_{cn}$ as expected for statistical evaporation from the complete fusion compound nucleus. Almost certainly, the heaviest products in each case are formed predominantly by evaporation following complete fusion.

Clearly, then, a process or processes involving significantly lower momentum transfer contributes to formation of the lighter products. The precise nature of such processes, and the resulting mix of competing processes, cannot be uniquely determined from these results. However, one class of mechanism which could account for this behavior is incomplete fusion[23,24] in which only part of the projectile fuses with the target while the remainder escapes with essentially beam velocity in a forward direction.

The mass yields from complete fusion are expected to be peaked between $A=101$ and 108 from 142 MeV ^{22}Ne, between 100 and 106 from 142 MeV ^{20}Ne, and between 105 and 109 from 100 MeV ^{20}Ne. While accurate determination of relative mass yields was not possible in the present work due to the presence of stable nuclides (not detected) and of many isomers which render the decay curves exceedingly complex, it appears that the actual mass yields, especially for the second and third of these cases, are flatter and extend to lower masses than expected from complete fusion.

To account for the steady variation in $\bar{v}_{||}$ over the interval from $A=105$ down to $A=96$, it is postulated that a succession of different processes, involving steadily decreasing transfer of mass and excitation energy, is responsible for forming these products. The diagonal dashed lines in Fig. 4 show the recoil velocity that an intermediate of mass A would have if formed by an incomplete fusion process in which the remainder of the projectile acted purely as a spectator. Products from such a process would give values of $\bar{v}_{||}$ lying to the left of the line by an amount equal to the subsequent mass evaporation from the intermediate. The 142 MeV ^{22}Ne and 100 MeV ^{20}Ne results are certainly consistent with such a picture. This does not imply, however, that the processes involved are actually as simple as this or that only a single such process contributes to formation of each.

It appears that complete fusion is relatively much more important for 142 MeV ^{20}Ne than for either of the other two sets of data. In the 142 MeV ^{20}Ne data, a "plateau" is seen for the heaviest products, from about mass 105 up; their production is apparently dominated by complete fusion. No similar plateau is seen in the other two cases, indicating that other processes compete effectively with complete fusion even in forming the heaviest products; this in turn implies that complete fusion is less important in these cases.

It should be noted that none of the preceding arguments will be significantly affected by the existence of feeding, which would mean that in some cases the measured ranges correspond not to the observed nuclide but to its β-decay parent.

The 100 MeV ^{22}Ne data have more scatter than the other data but are apparently anomalous, in that these include the only points that lie below the diagonal incomplete fusion line. These results are hard to explain, but clearly indicate that the mechanism is not complete fusion. Almost certainly, the two additional neutrons in ^{22}Ne are "lost" in the initial stages of the interaction.

B. Products with $A \leq 96$

The products with $A \leq 96$ were found in the backward catcher as well as the forward catcher, implying distribu-

tions of recoil angle extending beyond 45°. Clearly these products are formed in glancing collisions.

For each product, a value for the recoil angle $\bar{\alpha}_c$ (corrected as described in Sec. III for the effect of transverse straggling) was determined in addition to a value for $\bar{v}_{||}$, the mean longitudinal component of recoil velocity; these values are shown in Fig. 5. It is assumed that each product is formed by evaporation of a few nucleons from some corresponding intermediate, which recoiled with the same values of $v_{||}$ and α; using two-body kinematics, the energy and angle of emission of the accompanying projectilelike fragment(s) and the effective Q value of the first stage of the reaction can be deduced. The net excitation energy of intermediate and fragment(s) in this picture are obtained by comparing this effective Q value with the ground state Q value of the corresponding simple transfer reaction. If this excitation energy is greater than the binding energy of the single projectilelike fragment, further fragmentation may result.

Based on the deduced values of $v_{||}$ and α for a given product, energetically-forbidden intermediates and those with inappropriate excitation can then be eliminated. Such analysis has been applied to the results for $A \leq 96$ from the present work, and the conclusions are set out in the following.

Because of the low beam intensity, backward catcher yields were too low to be determined in the 100 MeV ^{22}Ne experiment, so the sections which follow discuss only the other three experiments. The 142 MeV ^{20}Ne and ^{22}Ne results are quite similar and will be discussed together; the 100 MeV ^{20}Ne results show completely different behavior.

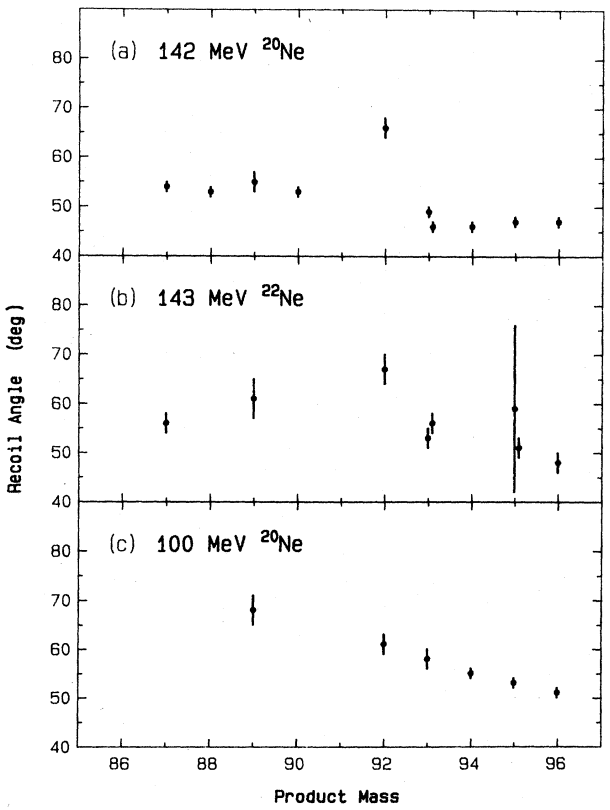

FIG. 5. Corrected "mean" recoil angle, measured for detected products from reactions of ^{20}Ne and ^{22}Ne with ^{93}Nb, as a function of product mass.

1. 142 MeV results

The results for products with $A \leq 96$ from 142 MeV ^{20}Ne and ^{22}Ne fall into three groups which show different behavior: (i) products with $93 \leq A \leq 96$, (ii) ^{92}Nb^m, and (iii) products with $A \leq 90$.

(a) Products with $93 \leq A \leq 96$. The observed products with masses in the range 93—96 comprise mainly the technetium isotopes. Transfer of a single α particle to the traget nucleus would form a ^{97}Tc* intermediate. In the 142 MeV ^{20}Ne experiment, all these products are found to have essentially identical values of $\bar{v}_{||}$ and $\bar{\alpha}_c$, suggesting that all are formed via the same intermediate. These values, approximately 0.31 v_{cn} and 47°, are kinematically consistent with the transfer process ^{93}Nb(^{20}Ne,^{16}O)^{97}Tc*, provided that the ^{16}O is emitted at a laboratory angle of about 22° with an energy, just below the beam velocity, of about 108 MeV, leaving an excitation energy of approximately 26 MeV. If this were confined to excitation of the ^{97}Tc* intermediate, it would be expected to lead to the subsequent evaporation of two or three nucleons; within the experimental uncertainties it is possible to account for evaporation of as few as one neutron or as many as four nucleons, so that all the observed products could be formed from this process. Thus it seems extremely probable that from 142 MeV ^{20}Ne, all the observed products with $93 \leq A \leq 96$ are formed by evaporation from a ^{97}Tc* intermediate formed by incomplete fusion in which only a single α particle fuses with the target.

The 142 MeV ^{22}Ne data have larger uncertainties, but are similar to the ^{20}Ne case, suggesting again that a ^{97}Tc* intermediate is involved: The two additional neutrons from ^{22}Ne accompany the projectilelike fragment, either bound as ^{18}O or as distinct fragments. The data are not consistent with a process in which ^{16}O is emitted and the two extra neutrons plus an α particle fuse with the target.

(b) ^{92}Nb^m. The values of $\bar{\alpha}_c$ obtained for ^{92}Nb^m ($\sim$66°) are significantly larger than for any other product at 142 MeV, indicating that this product is formed in glancing collisions at a large impact parameter, involving very little transfer of mass between projectile and target. Furthermore, ^{92}Nb^m is the only product observed for which the low-spin isomer was detected in measurable quantities.

The two processes most likely to be responsible for formation of ^{92}Nb^m from ^{93}Nb are knockout of a single neutron and inelastic scattering followed by evaporation of a neutron. The observed recoil quantities are consistent with either process, but the lack of production of the high spin isomer favors the former mechanism. If inelastic scattering were responsible, the values of $\bar{\alpha}_c$ and $\bar{v}_{||}$ obtained imply an available excitation of approximately 21 MeV, which is considerably more than required to evaporate one neutron from ^{93}Nb (the neutron separation energy is 8.8 MeV) so that sufficient excitation is available to break up the scattered ^{20}Ne (for example into ^{16}O + α).

We therefore conclude that ^{92}Nb^m is formed more likely

by neutron knockout but possibly by evaporation of one neutron from ^{93}Nb excited in an inelastic scattering process in which the scattered ^{20}Ne probably fragments. In either case, kinematics imply an outgoing angle for the center of mass of the fragment distribution of about 20°.

(c) Products with $A \leq 90$. Limited data were obtained for products below the target mass. The products observed with $A \leq 90$ from the 142 MeV ^{20}Ne experiment have essentially identical values of $\bar{\alpha}_c$ (about 53°) and values of $\bar{v}_{||}$, which perhaps increase with decreasing mass. These results cannot be explained on the basis of either evaporation following α particle transfer to the target (the recoil values imply much too low a value for the excitation of the ^{97}Tc* intermediate) or direct "cold" pickup (which would give much larger values of α). These products are probably formed by evaporation from excited intermediates with mass 93—90, formed by inelastic scattering or preequilibrium events, possibly involving pickup of a few nucleons by the projectilelike fragment (although the possibility of formation of the product with little excitation energy, accompanied by a highly-excited projectilelike fragment, cannot be ruled out). Thus the observed production of ^{90}Nb could be explained by evaporation of three neutrons following inelastic scattering of ^{20}Ne (the recoil values imply an available excitation energy of approximately 40 MeV), whereas the lighter products probably come from a slightly lighter intermediate (such as ^{91}Nb* formed by preequilibrium or pickup processes).

The data for the two such products observed from 142 MeV ^{22}Ne have large uncertainties, but are apparently similar to the corresponding ^{20}Ne results.

2. 100 MeV ^{20}Ne results

The 100 MeV ^{20}Ne data show completely different behavior from the 142 MeV data. Over the entire set of products observed with $A \leq 96$, from $A = 96$ down to $A = 89$, the value of $\bar{v}_{||}$ decreases monotonically and the value of $\bar{\alpha}_c$ increases monotonically. This can only be explained if each product is assumed to be formed via a rather "cold" transfer process, involving in each case an intermediate at most one mass unit heavier than the product, formed with just sufficient excitation to evaporate at most one nucleon, and leaving insufficient excitation in the outgoing projectilelike fragment for further breakup.

Thus formation of ^{96}Tc probably involves a ^{97}Tc* intermediate with emission of ^{16}O, ^{94}Tc probably a ^{95}Tc* intermediate with emission of ^{18}O, ^{93}Mo probably a ^{94}Mo* intermediate with emission of ^{19}F, and ^{89}Zr probably a ^{90}Zr* intermediate with emission of ^{23}Na. These projectilelike fragments would be emitted cold at angles ranging from 35° (for ^{16}O leading to ^{96}Tc) to 20° (for ^{23}Na).

In principle, the observed yield of ^{94}Tc could have been fed by ^{94}Ru, and ^{89}Zr by ^{89}Nb. However, it is impossible in any way to account for the observed recoil values assuming these to have been the products. Hence, it is assumed that feeding was not important for these nuclides. The other nuclides listed certainly cannot be fed.

It is perhaps significant that ^{93}Tc, which could not easily be formed in such a cold process (since its formation involves the transfer of two protons from projectile to target and the loss of two neutrons from the target), was not observed as a product from 100 MeV ^{20}Ne.

C. Isomer production

Isomers abound throughout the mass region studied in these experiments. Of the thirty-five nuclides for which recoil properties are reported here, twenty-six are isomeric states. However, in no case were the yields of both members of an isomeric pair sufficient for the ranges of both members to be measured. Indeed, in most cases the decay curves showed no evidence whatsoever of production of the low-spin isomer; only in the cases of ^{93,94}Tc was there an indication of measurable activity, and this was too low for accurate measurements due to the preponderance of the ground state decay. The gamma rays corresponding to several isomers which decay by isomeric transitions, including ^{95}Tc^m and ^{95}Nb^m, were not observed at all, while in other cases there was no evidence for the presence of two components (growth and decay) in the variation with time of a particular gamma-ray intensity.

The lack of production of low-spin isomers in either the Tc isotopes, or the higher-mass Ag isotopes, in the present work, is consistent with the previous observations of Shaw and Smith,[18,19] who were able to measure only a single isomer ratio (18—20 for ^{95}Tc^m/^{95}Tc^g) for ^{20}Ne incident upon ^{93}Nb at energies higher than those of the present work.

Although it was disappointing that isomer ratio determinations proved impossible, the observed dramatic preponderance of high-spin isomers is itself interesting.

V. SUMMARY AND CONCLUSIONS

For processes involving large momentum transfer and small recoil angles, the projected (longitudinal) recoil velocity is sufficient to characterize the reaction mechanism, but, for glancing processes with low momentum transfer and large recoil angles, mechanistic interpretation requires additional knowledge of the transverse momentum transfer or the recoil angle. The technique used in this work enables simultaneous determination of both the mean projected recoil velocity and a mean recoil angle for each product. Then, if one assumes a particular intermediate, the energy and angle of emission of the projectilelike fragment(s) and the excitation energy of the intermediate state can be calculated, and hence some processes eliminated on energetic grounds. In this way, specific conclusions have been reached in the study of reactions of ^{20}Ne and ^{22}Ne on ^{93}Nb.

With 142 MeV ^{20}Ne, the products with $93 \leq A \leq 96$ are formed by evaporation from an excited ^{97}Tc* intermediate formed by transfer of a single α particle to the target, in a process such as incomplete fusion. The products above mass 104 are predominantly formed by complete fusion followed by evaporation. Between mass 96 and mass 104, the average momentum transfer increases steadily; it is likely that varying admixtures of several processes involv-

ing different degrees of mass, and hence momentum, transfer contribute to forming these products. The lightest observed products ($A < 90$) are probably formed by successive evaporation of several particles from highly excited intermediates such as $^{93-91}$Nb, formed by inelastic scattering, or preequilibrium processes (with or without pickup of a few nucleons). ^{92}Nb^{m} is probably formed by neutron knockout, or possibly by evaporation following inelastic scattering (possibly with breakup of the scattered ^{20}Ne).

For 142 MeV ^{22}Ne, the data for low mass products are rather similar to those from ^{20}Ne (although with greater statistical uncertainty), suggesting that in the processes responsible for production of near-target products, the two additional neutrons accompany the projectilelike fragment (either bound or unbound). The contribution of complete fusion to the heavier products is apparently much less for 142 MeV ^{22}Ne than for ^{20}Ne, a significant result in view of the two valence neutrons of ^{22}Ne.

The 100 MeV ^{20}Ne results are dramatically different from the results at 142 MeV. Not only is the contribution from complete fusion relatively less important, but all the products below mass 96 are apparently formed in relatively cold transfer processes, involving intermediates with sufficient excitation for subsequent evaporation of at most one nucleon. The recoil results and kinematic calculations imply that the projectilelike fragment is emitted in each case at an angle near 20°.

The limited data obtained with 100 MeV ^{22}Ne are anomalous and hard to explain, but are certainly not consistent with complete fusion.

ACKNOWLEDGMENTS

The authors wish to acknowledge the help of Mr. E. J. Jones and the operating staff of the VEC, Harwell, in the preparation of the ^{22}Ne beam. Encouragement for this work came from Professor E. Gadioli, Dr. T. W. Conlon, and Dr. P. E. Hodgson, with all of whom helpful discussions of its interpretation were held. The unpublished Manchester data were kindly made available to us by Dr. R. Smith and Dr. E. Shaw. This work was made possible by an International Scientific Exchange grant, jointly administered by the Natural Science and Engineering Research Council of Canada and the Royal Society, London, as well as by a travel grant from the British Council.

[1]Early work is reviewed by A. Zucker and K. S. Toth, in *Nuclear Chemistry,* edited by L. Yaffe (Academic, New York, 1968).

[2]D. K. Scott, in *Theoretical Methods in Medium-Energy and Heavy-Ion Physics,* Proceedings of a NATO Advanced Studies Institute, University of Wisconsin, Madison, 1978 [NATO Advanced Studies Institute Series B (Physics), Vol. 38], edited by K. W. McVoy and W. A. Friedman (Plenum, New York, 1978).

[3]P. E. Hodgson, *Heavy Ion Reactions* (Oxford University Press, New York, 1978).

[4]J. R. Birkelund and J. R. Huizenga, Phys. Rev. C **17**, 126 (1978).

[5]M. El-Nadi and A. Hasham, Phys. Rev. C **23**, 2586 (1981).

[6]M. Blann, Phys. Rev. C **21**, 1770 (1980).

[7]F. S. Stephens, in *Proceedings of the International Conference on Nuclear Structure, Berkeley, California, 1980,* edited by R. M. Diamond and J. O. Rasmussen (North-Holland, Amsterdam, 1981), p. 289.

[8]First work: S. Kaufmann and R. Wolfgang, Phys. Rev. **121**, 192 (1961).

[9]Recent review: W. U. Schröder and J. R. Huizenga, Annu. Rev. Nucl. Sci. **27**, 465 (1977).

[10]M. Blann, Phys. Rev. C **23**, 205 (1981).

[11]T. C. Awes, S. Saini, G. Poggi, C. K. Gelbke, D. Cha, R. Legrain, and G. D. Westfall, Phys. Rev. C **25**, 2361 (1982).

[12]J. M. Alexander, in *Nuclear Chemistry,* edited by L. Yaffe (Academic, New York, 1968), Chap. 4.

[13]D. Gardes, R. Bimbot, J. Maison, M. F. Rivet, A. Fleury, F. Hubert, and Y. Llabador, Phys. Rev. C **21**, 2447 (1980), and many previous papers.

[14]G. D. Cole and N. T. Porile, Phys. Rev. C **25**, 244 (1982).

[15]D. J. Parker, J. Asher, T. W. Conlon, and I. Naqib, Phys. Rev. C **30**, 143 (1984).

[16]J. Wilczynski, Nucl. Phys. **A216**, 386 (1973); Phys. Lett. **47B**, 484 (1973).

[17]R. Bass, Phys. Lett. **47B**, 139 (1973).

[18]E. Shaw, Ph.D. thesis, University of Manchester, 1982.

[19]R. Smith, Ph.D. thesis, University of Manchester, 1982.

[20]L. C. Northcliffe and R. F. Schilling, Nucl. Data Tables **A7**, 233 (1970).

[21]U. Reus, W. Westmeier, and I. Warnecke, Gesellschaft für Schwerionenforschung Gamma Ray Catalog, Report GSI-79-2, 1979.

[22]U. Littmark and J. F. Ziegler, *The Stopping and Ranges of Ions in Matter* (Pergamon, New York, 1977), Vol. 6.

[23]C. Gerschel, Nucl. Phys. **A387**, 297c (1982).

[24]R. H. Siemssen, Nucl. Phys. **A400**, 245c (1983).